Electrochemical Fabrication of Large-Area, Ordered Bi₂Te₃ Nanowire Arrays

Chuangui Jin,[†,‡] Xiaoqiang Xiang,[†] Chong Jia,[†] Weifeng Liu,[†] Weili Cai,[†] Lianzeng Yao,[†] and Xiaoguang Li*,[†]

Structure Research Laboratory, Department of Materials Science and Engineering, University of Science and Technology of China, Hefei 230026, P. R. China, and College of Chemical Engineering and Environment, Anhui University of Technology, Maanshan 243002, China

Received: July 22, 2003; In Final Form: November 23, 2003

Thermoelectric material Bi₂Te₃ has been successfully synthesized by cathodic electrolysis into porous anodic alumina membranes. X-ray diffraction (XRD), high-resolution transmission electron microscopy (HRTEM), and electron diffraction (ED) results show that the as-synthesized samples are hexagonal Bi₂Te₃ single-crystal nanowires. The morphologies and structure of the Bi₂Te₃ nanowires have been characterized using scanning electron microscopy (SEM) and transmission electron microscopy (TEM). The results demonstrate that the Bi₂Te₃ nanowire arrays with a high-filling rate and a large area are dense, continuous, and smooth. Energy dispersive spectrometer (EDS) analysis indicates that the atomic ratio of Bi to Te is very close to 2:3 stoichiometry.

Introduction

Recently, one-dimensional nanostructured materials such as nanowires, nanorods, nanobelts, and nanotubes have become the focus of intensive research due to their unique applications in mesoscopic physics and fabrication of nanoscale devices.[1−2] Among various approaches to prepare nanowires, much attention has been paid to the anodic alumina membrane (AAM)-based synthesis in conjunction with the electrochemical deposition because the AAM templates possess a uniform and parallel porous structure, and the electrochemical deposition technique is relatively simple and inexpensive, which provides an exquisite way to prepare highly ordered nanowire arrays. Therefore, nanowires of metals,[3−6] alloys,[7−12] and semiconductors[13−15] have been fabricated within the pores of the anodic alumina membranes using the electrochemical deposition technique.

Bismuth telluride (Bi₂Te₃)-based compounds have attracted a considerable interest as thermoelectric (TE) materials. The bulk Bi₂Te₃ has a high thermoelectric figure-of-merit and is widely used commercially. High-quality Bi₂Te₃ films have been prepared by electrochemical deposition in an acidic aqueous solution.[16] Theoretical studies show that Bi₂Te₃ nanowires may have a high figure-of-merit,[17−19] which is verified by Venkata-subramanian et al.[20] Stacy's group[21−23] has prepared Bi₂Te₃ nanowire arrays with different diameters by potentiostat electrochemical deposition into the nanochannels of the porous anodic alumina template. It is still a challenge, however, to fabricate high-filling, high-aspect ratio, large-area, uniform, and single-crystal nanowire arrays. In this article, large-area, continuous, and ordered Bi₂Te₃ nanowire arrays have been successfully prepared using the electrochemical deposition technique by controlling the solution concentrations, the current density, and the pH.

Experimental Section

The AAM was fabricated in a two-step anodization process as described in the literature.[24−25] After the second anodization, the remaining aluminum was etched by 1 M CuCl₂ solution. The alumina barrier layer was then dissolved, and the pores were widened using 5 wt % H₃PO₄ solution at room temperature for ~1−2 h. Finally, a layer of Au film was sputtered onto one side of the through-hole AAM template to serve as the working electrode in a two-electrode electrochemical cell, and a graphite plate was used as the counter electrode. Bi₂Te₃ nanowires were electrochemically deposited at a constant current density of 2.5 mA/cm² for 2 h in a glass cell at room temperature, which was strictly controlled by a potentiostat/galvanostat (HDV-7C). The electrolyte solution consisted of 0.035 M Bi (NO₃)₃·5H₂O and 0.05 M HTeO₂⁺. The HTeO₂⁺ came from the reaction of Te powder to 5 M HNO₃. The pH of the solution was adjusted to 1 by adding 1 M HNO₃ solution. After deposition, the AAM template with Bi₂Te₃ nanowires was rinsed with absolute ethanol and then dried in air at room temperature for further analysis.

The overfilled nanowires on the surface of the AAM template and the back Au film were carefully swept out with superfine Al₂O₃ powder for X-ray diffraction (XRD), transmission electron microscopy (TEM), and high-resolution transmission electron microscopy (HRTEM) studies. XRD of the nanowire arrays was performed on an X-ray diffractometer (D/MAX-γA) with Cu Kα radiation in the range of 10° ≤ 2θ ≤ 70°. The morphology of the as-synthesized AAM template and the Bi₂Te₃ nanowire arrays was observed using a field emission scanning electron microscope (JEOL JSM-6700F) and a transmission electron microscope (H-800). For scanning electron microscopy (SEM) observations, the AAM template was partly dissolved with 1 M NaOH solution. The residual solution on the surface of the AAM template was carefully rinsed with distilled water several times. For TEM observations, the AAM template was completely dissolved in a 2 M NaOH aqueous solution, which was thoroughly washed with distilled water to remove residual NaOH, and then the sample was slowly rinsed with absolute ethanol. The HRTEM (JEOL-2010) and electron diffraction

* Corresponding author. Tel: +86-551-3603408. Fax: +86-551-3603408. E-mail: lixg@ustc.edu.cn.
† University of Science and Technology of China.
‡ Anhui University of Technology.

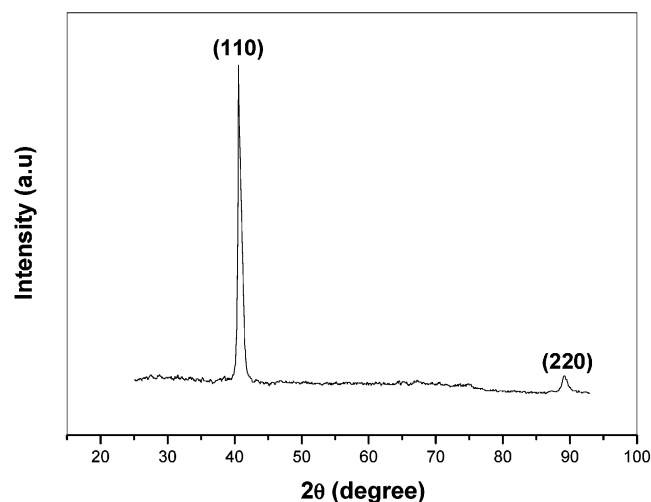Fabrication of Bi₂Te₃ Nanowire Arrays

J. Phys. Chem. B, Vol. 108, No. 6, 2004 **1845**

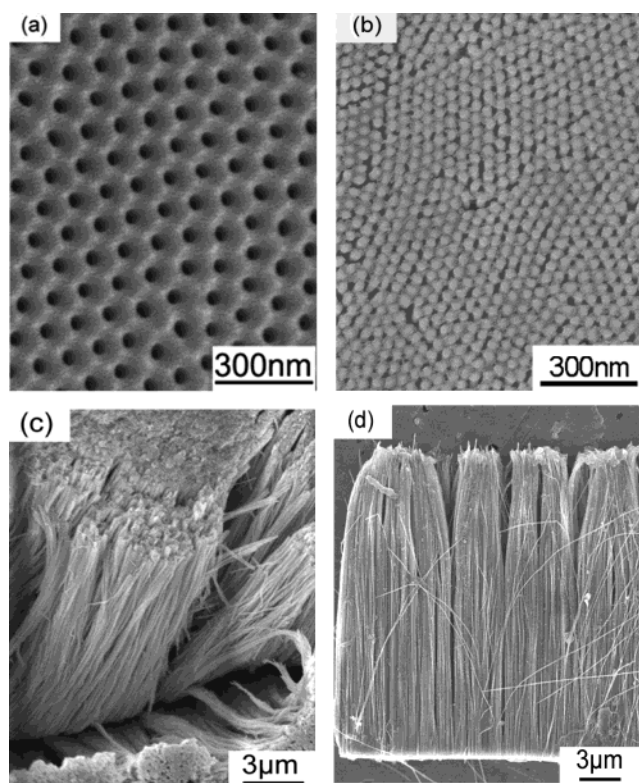**Figure 1.** XRD pattern of Bi₂Te₃ nanowire arrays (electrodeposition time: 5 min).

Figure 2. SEM photographs of AAM template and Bi₂Te₃ nanowire arrays. (a) A typical SEM photograph of AAM. (b) Surface view of Bi₂Te₃ nanowire arrays (eroding time: 5 min). (c) Surface view of Bi₂Te₃ nanowire arrays (eroding time: 15 min). (d) Cross-sectional view of Bi₂Te₃ nanowire arrays (eroding time: 15 min).

(ED) attached to the HRTEM were employed to characterize the nanowires' crystal structure. The chemical composition of the nanowire arrays was determined by an energy dispersive spectrometer (EDS) attached to the HRTEM.

Results and Discussion

The XRD pattern of the as-prepared sample is shown in Figure 1. Only (110) and (220) peaks of the hexagonal Bi₂Te₃ (JCPDS, 15-863) can be seen clearly. It indicates that the preferred growth direction for the Bi₂Te₃ nanowires is the [110] direction, which is verified by the HRTEM result. In addition, no diffraction peaks from the elemental Bi and Te are detected.
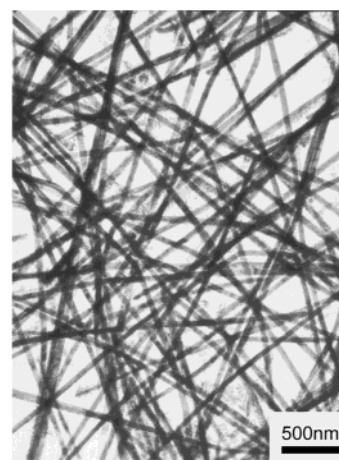

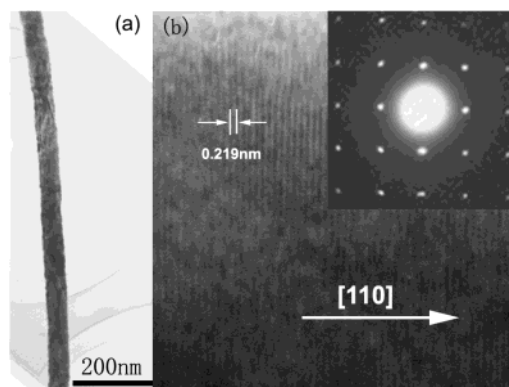**Figure 3.** TEM image of Bi₂Te₃ nanowires.

Figure 4. TEM and HRTEM images of a single Bi₂Te₃ nanowire. (a) TEM image and (b) HRTEM image of the same nanowire. The inset is the corresponding ED pattern.

The morphologies of the as-prepared AAM template and the Bi₂Te₃ nanowire arrays are shown in Figure 2. Figure 2a is a typical SEM image of the as-prepared AAM template. Highly ordered pores with a diameter about 50 nm and an interpore distance around 100 nm can be seen from Figure 2a. The surface view of the nanowire arrays after etching is presented in Figure 2b,c. Apparently, all the pores are filled with nanowires, and the exposed parts of the nanowires increase as the eroding time increases, as shown in Figure 2b,c. Figure 2d is the cross-sectional view of the Bi₂Te₃ nanowire array with a length as long as tens of micrometers. Because the electrodeposition follows a bottom-up mechanism, the deposition of Bi₂Te₃ nanowires starts at the Au cathode on the bottom of the pores, and then the Bi₂Te₃ nanaowires grow along the pores to the top. Therefore, the length of Bi₂Te₃ nanowires is the same as the thickness of the anodic alumina template used.

Figure 3 is a typical TEM image of the Bi₂Te₃ nanowires. Large amounts of the nanowires with a smooth and clean surface and a high-aspect ratio can be seen from Figure 3. The diameters are uniform and the same as those of the nanochannels of the AAM template used.

A typical HRTEM image of a single Bi₂Te₃ nanowire and corresponding ED pattern are displayed in Figure 4. From the HRTEM image of it, it can be seen that the nanowire is dense and uniform in diameter. The HRTEM lattice fringes are perpendicular to the axis of the nanowires and show an interplanar spacing of about 0.219 nm, which is consistent with the interplanar distance of the {110} planes ($d = 0.219$ nm) of the bulk hexagonal Bi₂Te₃. It indicates that the growth direction is along the ⟨110⟩ direction, which is in agreement with the
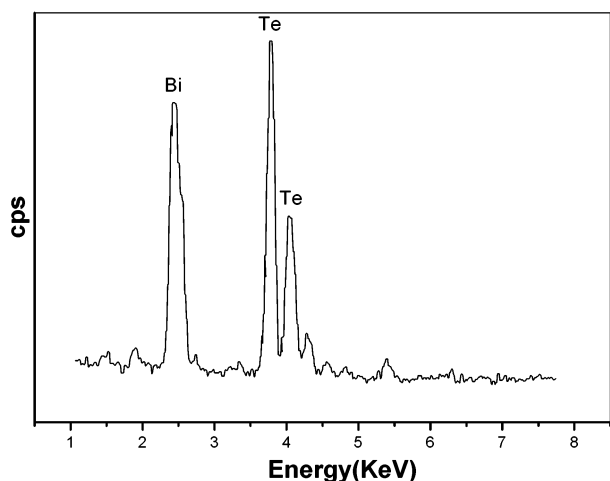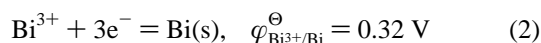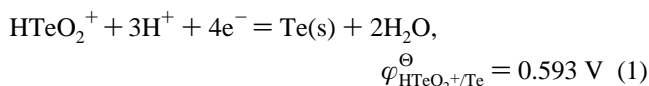
Figure 5. EDS of Bi_2Te_3 nanowires.

XRD result. The HRTEM and ED results demonstrate that the Bi_2Te_3 nanowires are single crystals.

The EDS result of the nanowire is presented in Figure 5, which verifies that the nanowires consist of Bi and Te, and quantitative analysis of the spectrum indicates that the atomic ratio of Bi to Te is close to 2:3.

The electrodeposition process of the Bi_2Te_3 nanowires mainly involves the following steps. First, the $HTeO_2^+$ and Bi^{3+} diffuse to the Au electrode surface and adsorb on the surface by the electric field force. Second, the adsorbed $HTeO_2^+$ and Bi^{3+} get electrons to produce elemental Te and Bi by the following reactions:[26]

$$HTeO_2^+ + 3H^+ + 4e^- = Te(s) + 2H_2O,$$
$$\varphi_{HTeO_2^+/Te}^{\ominus} = 0.593 \text{ V} \quad (1)$$

$$Bi^{3+} + 3e^- = Bi(s), \quad \varphi_{Bi3+/Bi}^{\ominus} = 0.32 \text{ V} \quad (2)$$

where $\varphi_{HTeO_2^+/Te}^{\ominus}$ is the standard electrode potential of the $HTeO_2^+$ and Te half cell reaction, $\varphi_{Bi3+/Bi}^{\ominus}$ is the standard electrode potential of the Bi^{3+} and Bi half cell reaction. The half cell reaction conditions are pressure at 14.706 psi and temperature at 298.15 K; all matters activities are 1.[27] Third, the elemental Te reacts with Bi to form Bi_2Te_3.

Thus, the overall reaction can be expressed as:

$$3HTeO_2^+ + 9H^+ + 18e^- + 2Bi^{3+} = Bi_2Te_3(s) + 6H_2O \quad (3)$$
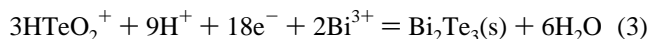
To prepare large-area, single-crystal, and stoichiometric Bi_2Te_3 nanowire arrays, some factors should be considered. First, according to the Nerst equation:

$$\varphi_{HTeO_2^+/Te} = \varphi_{HTeO_2^+/Te}^{\ominus} + \frac{RT}{n_1F} \ln \frac{[a_{(HTeO_2^+)}][a_{(H^+)}]^3}{[a_{(Te)}]} \quad (4)$$

$$\varphi_{Bi3+/Bi} = \varphi_{Bi3+/Bi}^{\ominus} + \frac{RT}{n_2F} \ln \frac{[a_{(Bi3+)}]}{[a_{(Bi)}]} \quad (5)$$

where R is the gas constant, $R = 8.314 J \text{ mol}^{-1} \text{ K}^{-1}$; F is the Faraday constant, $F = 96487C \text{ mol}^{-1}$; n_1 and n_2 are the numbers of the gaining electrons of the half cell reaction, $n_1 = 4$, $n_2 = 3$; and T is the temperature of half cell reaction, $T \approx 298.15$ K. The activities of the pure solids are 1, ion molar concentrations are approximately equal to ion activities in the dilute solution. Therefore, because $a_{(HTeO_2^+)} \approx c_{(HTeO_2^+)} = 0.05$ M, $a_{(Bi3+)} \approx c_{(Bi3+)}$

$= 0.035$ M, $a_{(Te)} = a_{(Bi)} = 1$, $c_{(H^+)} \approx a_{(H^+)} = 1$ and because we can calculate the $\varphi_{HTeO_2^+/Te} = 0.574$ V, $\varphi_{Bi3+/Bi} = 0.291$ V from the Nerst equation, it is evident that pH can affect $\varphi_{HTeO_2^+/Te}$. On one hand, the $\varphi_{HTeO_2^+/Te}$ and the $\varphi_{Bi3+/Bi}$ values are also higher than the φ_{H^+/H_2} value, but on the other hand, H_2 has high overpotential, which is why it is impossible to produce H_2 on the cathode. If it happened, the formed H_2 bubbles would hinder the $HTeO_2^+$ and the Bi^{3+} from diffusing toward the surface of Au electrode, which would make it difficult to prepare high-filling, continuous nanowires. Besides, strong acid solution can prevent the $HTeO_2^+$ and the Bi^{3+} from hydrolyzing. Second, to grow nanowires simultaneously in as many pores as possible, we tried to minimize the growth rate by reducing the concentrations of $HTeO_2^+$ and Bi^{3+} because high ion concentrations will cause a rapid nucleation, rapid growth, and a concentration gradient which is unfavorable for producing dense and single-crystal nanowires. Third, the dc electrodeposition process is favorable to form steady diffusion and, thus, to produce high-quality Bi_2Te_3 nanowires, whereas, for the ac process, the diffusion rate and the direction will change with the alternative electric field, resulting in a few polycrystalline nanowires with a high density of defects.[28-29] Fourth, to fabricate stoichiometric Bi_2Te_3 nanowires, $2Bi^{3+}$ and $3HTeO_2^+$ should be deposited simultaneously, which is achieved by choosing a suitable current density because the current density can affect the ion diffusion rate. In our experiments, the stoichiometric Bi_2Te_3 nanowires can be prepared only at 2.5 mA/cm^2.

Conclusion

In conclusion, high-filling, uniform, single-crystal Bi_2Te_3 nanowire arrays have been prepared by direct-current electrodeposition into the pores of AAM template at room temperature. The optimum conditions under which high-filling, uniform, and single-crystal Bi_2Te_3 nanowire arrays can be prepared are also discussed. If we understand well the nature of high-filling, ordered single-crystal metal nanowire arrays made by using the electrochemical deposition technique, it will help us to synthesize other metal, semimetal, or semiconductor single-crystal nanowire arrays using the same technique.

References and Notes

(1) Wang, Z. L. *Adv. Mater.* **2000**, *12*, 129.
(2) Hu, J.; Odom, T. W.; Lieber, C. M. *Acc. Chem. Res.* **1999**, *32*, 435.
(3) Sauer, G.; Brehm, G.; Schneider, S.; Nielsh, K.; Gösele, U. *J. Appl. Phys.* **2002**, *91*, 3243.
(4) Choi, J.; Sauer, G.; Nielsh, K.; Wehrspohn, R.; Gösele, U. *Chem. Mater.* **2003**, *15*, 776.
(5) Zhang, Y.; Li, G. H.; Wu, Y. C.; Zhang, B.; Song, W. H.; Zhang, L. D. *Adv. Mater.* **2002**, *17*, 1227.
(6) Sellmyer, D. J.; Zheng, M.; Skomski, R. *J. Phys.: Condens. Matter* **2001**, *13*, R433.
(7) Guo, Y. G.; Wan, L. J.; Zhu, C. F.; Yang, D. L.; Chen, D. M.; Bai, C. L. *Chem. Mater.* **2003**, *15*, 664.
(8) Khan, H. R.; Petrikowski, K. *J. Magn. Magn. Mater.* **2000**, *215*, 526.
(9) Qin, D. H.; Cao, L.; Sun, Q. Y.; Huang, Y.; Li, H. L. *Chem. Phys. Lett.* **2002**, *358*, 484.
(10) Wang, Y. W.; Zhang, L. D.; Meng, G. W.; Peng, X. S.; Jin, Y. X.; Zhang, J. *J. Phys. Chem. B* **2002**, *106*, 2502.
(11) Prieto, A. L.; González, M. M.; Keyani, J.; Gronsky, R.; Sands, T.; Stancy, A. M. *J. Am. Chem. Soc.* **2003**, *125*, 2388.
(12) Fodor, P. S.; Tsoi, G. M.; Wenger, L. E. *J. Appl. Phys.* **2002**, *15*, 8186.
(13) Xu, D. S.; Shi, X. S.; Guo, G. L.; Gui, L. L.; Tang, Y. Q. *J. Phys. Chem. B* **2000**, *104*, 5061.

(14) Wang, Y. C.; Leu, I. C.; Hon, M. H. *J. Cryst. Growth* **2002**, *23*, 564.

(15) Peng, X. S.; Zhang, J.; Wang, X. F.; Zhang, L. D. *Chem. Phys. Lett.* **2001**, *343*, 470.

(16) Miyazaki, Y.; Kajitani, T. *J. Cryst. Growth* **2001**, *229*, 542.

(17) Dresselhaus, M. S.; Dresselhaus, G.; Sun, X.; Zhang, Z.; Cronin, S. B.; Koga, T. *Phys. Solid State* **1999**, *41*, 679.

(18) Hicks, L. D.; Dresselhaus, M. S. *Phys. Rev. B* **1993**, *47*, 16631.

(19) Dresselhaus, M. S.; Dresselhaus, G.; Sun, X.; Zhang, Z.; Cronin, S. B.; Koga, T.; Ying, J. Y.; Chen, G. *Microscale Thermophys. Eng.* **1999**, *3*, 89.

(20) Venkatasubramanian, R.; Siivola, E.; Colpitts, T.; Quinn, B. O. *Nature* **2001**, *413*, 597.

(21) Prieto, A. L.; Sander, M. S.; Marisol, S.; González, M.; Gronsky, R.; Sands, T.; Stacy, A. M. *J. Am. Chem. Soc.* **2001**, *123*, 7160.

(22) Sander, M. S.; Prieto, A. L.; Gronsky, R.; Sands, T.; Stacy, A. M. *Adv. Mate*r. **2002**, *9*, 665.

(23) Sander, M.; Gronsky, S. R.; Stacy, A. M. *Chem. Mater.* **2003**, *15*, 335.

(24) Masuda, H.; Fukuda, K. *Science* **1995**, *268*, 1466.

(25) Masuda, H.; Hasegwa, F.; Ono, S. *J. Electrochem. Soc.* **1997**, *144*, L127.

(26) Miyazaki, Y.; Kajitani, T. *J. Cryst. Growth* **2001**, *229*, 542.

(27) Weast, R. C.; Lide, D. R.; Astle, M. J.; Beyer, W. H. *Handbook of Chemistry and Physics*; CRC Press: Boca Raton, FL, 1989.

(28) Routkevitch, D.; Bigioni, T.; Moskovits, M.; Xu, J. M. *J. Phys. Chem.* **1996**, *100*, 14037.

(29) Hutchison, J. L.; Routkevitch, D.; Moskovits, M.; Nayak, R. R. *Inst. Phys. Conf. Ser.* **1997**, *157*, 389.